DOI: 10.1002/zaac.201200301

The Structural Chemistry of Quaternary Chalcogenides of the Type AMM'Q_3

Lukasz A. Koscielski[a] and James A. Ibers*[a]

Keywords: Quaternary chalcogenides; Structure types; Lanthanide compounds; Actinide compounds

Abstract. The rich structural chemistry of compounds of the type AMM'Q_3, where A is an *s*-block alkali- or alkaline-earth metal, M is a *d*-block transition metal, M' is another *d*-block metal or an *f*-block metal, and Q is a chalcogen, is discussed. We briefly consider the syntheses and physical property measurements of these compounds, but our main emphasis is on differences and trends among the seven structure types in which the 160 known, structurally characterized compounds crystallize.

Introduction

Compounds of the formula AMM'Q_3 comprise a large family of approximately 160 known compounds that have been characterized structurally. Here, A is an *s*-block alkali- or alkaline-earth metal, M is a *d*-block transition metal, M' is another *d*-block metal or an *f*-block metal, and Q is a chalcogen. These compounds crystallize in seven different structure types, namely those of $KCuZrS_3$,[1] Eu_2CuS_3 (i.e. $Eu^{2+}Cu^{1+}Eu^{3+}(S^{2-})_3$),[2] Ba_2MnS_3,[3] $BaCuLaS_3$,[4] $BaAgErS_3$,[5] $NaCuTiS_3$,[6] and $TlCuTiTe_3$.[7] Because there are no Q–Q bonds in these structures it is convenient to divide the compounds among three subtypes I, II, and III on the basis of the formal oxidation states of the atoms A, M, and M'. The three subtypes are: I, $A^{1+}M^{1+}M'^{4+}(Q^{2-})_3$; II, $A^{2+}M^{1+}M'^{3+}(Q^{2-})_3$; III, $A^{1+}M^{2+}M'^{3+}(Q^{2-})_3$. The 39 known compounds of subtype I (Table 1 and Supporting Information) crystallize in three different structure types, the 63 known compounds of subtype II (Table 2 and Supporting Information) crystallize in five different structure types, but the 58 compounds of subtype III (Table 3) crystallize in only one structure type, namely that of $KCuZrS_3$. Here we briefly discuss the syntheses and known physical properties of these compounds but our main emphasis is on differences and trends among their structures.

Syntheses

The syntheses of the AMM'Q_3 compounds tabulated in Tables 1–3 made use of standard high-temperature solid-state methods. The reactants consisted of the powdered elements that were almost always loaded inside an oxygen-free glove box into fused-silica tubes that were then evacuated to near 10^{-3} Torr, sealed, placed in a computer-controlled furnace, and heated according to specific temperature profiles. Maximum temperatures involved were between 673 and 1420 K. The reactions were slow cooled, rather than quenched. Generally, a low-melting flux, either an alkali-metal chalcogenide or more rarely an alkali-metal halide, was included in the loading to serve as a fluid medium in which the reagents could react. The flux was generally incorporated into the final product, hence the "reactive flux method."[8]

Physical Property Measurements

Physical measurements were performed on 63 of the 160 compounds. Many such measurements were carried out on powders, rather than single crystals. Particularly for magnetic measurements the use of powders can lead to erroneous results arising from the presence of impurities below the level of detection by X-ray powder diffraction measurements.

Magnetic Susceptibility

Magnetic susceptibility measurements were performed on two subtype I compounds,[9,10] 14 subtype II compounds,[11–14] and 26 subtype III compounds.[13,15–18] The effective magnetic moment, μ_{eff}, was calculated for each of these compounds and was in good agreement with theoretical values, supporting the presence of U^{4+} and Ln^{3+} ions. The compounds containing samarium were found not to follow the Curie–Weiss law.

Electrical Conductivity

Electrical conductivity measurements were only performed on five subtype I compounds. The reported measurements showed that $KCuZrS_3$ was an insulator, $KCuZrSe_3$ displayed

* Prof. J. A. Ibers
Fax: +1-847-491-2976
E-Mail: ibers@chem.northwestern.edu
[a] Department of Chemistry
Northwestern University
2145 Sheridan Road
Evanston, IL 60208–3113, USA

Supporting information for this article is available on the WWW under http://dx.doi.org/10.1002/zaac.201200301 or from the author.

Special Issue

Table 1. Subtype I compounds, $A^{1+}M^{1+}M'^{4+}Q^{2-}$. A box with a reference number indicates that the compound is known and has been structurally characterized. Structure type by cell background: $KCuZrS_3$ – white, $NaCuTiS_3$ – vertical lines, $TlCuTiTe_3$ – horizontal lines. Physical characterization: C – conductivity, M – magnetic, O – optical, T – theoretical. The A and M' elements are arranged in order of increasing crystal radii. A colored version may be found in the Supporting Information.

	M'	Ti	Hf		Zr	Np		U			Th
A	Q M	Cu	Cu	Ag	Cu	Cu	Ag	Cu	Ag	Au	Cu
Na	S	[6]			[6]						
	Se		[33]		[6]						
	Te				[6]						
K	S		[34]		[1] C	[35]	[35]	[19]			[20] O
	Se				[1] C			[9] C M O			[36]
	Te				[1] C						
Tl	S		[37]		[37]						
	Se		[37]		[37]						[38]
	Te	[7]									
Rb	S					[35]		[19] O	[19] O		
	Se								[19]	[10] M	
	Te			[39]						[10]	
Cs	S					[35]	[35]	[19] C O T	[19] C O T		
	Se				[13]			[13]	[19]	[10]	[36]
	Te							[26]		[10]	

Table 2. Subtype II compounds, $A^{2+}M^{1+}M'^{3+}(Q^{2-})_3$. A box with a reference number indicates that the compound is known and has been structurally characterized. Structure type by cell background: $KCuZrS_3$ – white, Eu_2CuS_3 – gray, Ba_2MnS_3 – crosshatch, $BaAgErS_3$ – vertical bars, $BaCuLaS_3$ – horizontal bars. Physical characterization: M – magnetic, O – optical. The A and M' elements are arranged in order of increasing crystal radii. A colored version may be found in the Supporting Information.

	A	Eu	Sr		Pb		Ba		
M'	M Q	S	S	Se	S	Se	S	Se	Te
Sc	Cu						[12]		
Lu	Cu	[11] M	[40]	[27]	[25]	[41]			
Yb	Cu	[11] M			[25]	[42]			[14]
Tm	Cu	[11] M			[25]	[41]			
Er	Cu				[25]	[41]	[12]	[12]	
	Ag						[5]	[12]	
Y	Cu	[11] M			[32]	[43]	[12] O	[12]	[14]
	Ag						[5]	[12]	[14]
Ho	Cu				[25]	[41]			
Dy	Cu	[11] M			[25]	[41]			[44]
Tb	Cu	[11] M			[25]	[41]			
Gd	Cu	[11] M	[40]	[27]		[41]	[12] M O	[13] M O	
	Ag						[5]		[14]
	Au							[14]	
Eu	Cu	[11] M							
Nd	Cu						[12] M O		[14]
	Ag						[12] O		[14] M
Pr	Cu			[28]					[14]
Ce	Cu			[28]			[12] M	[12] M	
La	Cu			[27]	[29]		[3]	[4] [12]	[14]
	Ag							[12]	[14]

metallic behavior down to 50 K where it underwent a transition to semiconducting behavior, $KCuZrTe_3$ was a metal,[1] and $KCuUSe_3$ and $CsCuUS_3$ were semiconductors.[9,19]

Optical Measurements

Compounds containing thorium are colored, those containing uranium and neptunium are black, those containing titanium, zirconium, and hafnium range from colored to black to metallic, and those containing lanthanides are colored.

Optical measurements (either absorbance or diffuse reflectance) were performed on six subtype I compounds,[9,19,20] five subtype II compounds,[12,14] and 22 subtype III compounds.[13,15,17,18,21] Face-dependent optical absorbances on single crystals of the subtype III compounds led to measured band gaps that are consistent with the colors of the compounds.

Zeitschrift für anorganische und allgemeine Chemie ZAAC Journal of Inorganic and General Chemistry

Table 3. Subtype III compounds $A^{1+}M^{2+}M'^{3+}(Q^{2-})_3$. A box with a reference number indicates that the compound is known and has been structurally characterized. All compounds are of the $KCuZrS_3$ structure type. Physical characterization: M – magnetic, O – optical, T – theoretical. The M and M' elements are arranged in order of increasing crystal radii.

	M'	Lu	Yb		Tm	Er	Y	Ho	Dy	Tb	Gd	Sm	Nd	Pr	Ce	La
M	Q A	Cs	Rb	Cs	Cs	Cs	Cs	Cs	Cs	Cs	Cs	Cs	Cs	Cs	Cs	Cs
Zn	S			[15] M O												
	Se		[15] M O	[16] M O	[16] M	[16] M O	[16] O T	[16] M	[16] M	[16] M	[13] M O	[16] M O				
	Te		[15]	[15]	[21]	[21]	[21]	[21]	[21]	[21] O	[21] O T	[21]	[21]	[21]		[21]
Mn	Se			[15] M O	[15] M	[15] M	[15]	[15] M	[15] M	[15] M	[15] M	[15]				
Hg	Se						[18] O T				[18] M O	[18] M O	[18]	[18]	[18] MO	[18] O
Cd	Se						[18] O T		[18] O	[18] O	[18] O	[18] O		[18]	[18] O	
	Te	[17]			[17] M O T	[17]		[17]	[17] M	[17]	[17] M	[17] M	[17] M	[17] M		[17]

Consistent with its ivory color the diffuse reflectance spectrum of $CsGdZnSe_3$ revealed two band gaps, one at 1.88 and the other at 2.92 eV.[13] The nature of the band gap in layered materials depends on a number of factors: the interlayer distance; the degree of interlayer van der Walls contact; the dimensionality and the relative covalency of features within a layer.[16, 20–22]

Theoretical Calculations

Periodic spin-polarized band-structure calculations were performed with the use of the first-principles DFT program VASP (Vienna ab initio Simulation Package)[23] for the subtype I compounds $CsCuUS_3$ and $CsAgUS_3$. The calculated values of the band gaps overestimated the experimental values by a factor of two, a typical result for 5*f* systems. Calculations of the magnetic structure showed an antiferromagnetic state to be lowest in energy.[19] DFT calculations on the subtype III compounds $CsMYSe_3$ (M = Zn, Cd, Hg) were carried out with the program WIEN2k.[24] The band gaps for $CsZnGdTe_3$, and $CsCdTmTe_3$ were in close agreement with experiment, but the band gap for the mercury compound was underestimated. The calculations indicated that these compounds are direct-gap semiconductors.[17,18,21]

Structure Types and the AMM'Q_3 Compounds

The structural results discussed here were almost always based on X-ray diffraction data collected on single crystals. There are a few instances where X-ray diffraction data from powders were used and one where neutron diffraction data were obtained.[15]

The compounds AMM'Q_3 crystallize in seven structure types, namely $KCuZrS_3$ (orthorhombic space group *Cmcm*), Eu_2CuS_3 (i.e. $Eu^{2+}Cu^{1+}Eu^{3+}(S^{2-})_3$) (orthorhombic space group *Pnma*), Ba_2MnS_3 (space group *Pnma*), $BaCuLaS_3$ (space group *Pnma*), $BaAgErS_3$ (monoclinic space group *C*2/*m*), $NaCuTiS_3$ (space group *Pnma*), and $TlCuTiTe_3$ (monoclinic space group $P2_1/m$). Subtype I compounds, i.e. those of formula $A^{1+}M^{1+}M'^{4+}(Q^{2-})_3$, crystallize in either the $KCuZrS_3$, the $NaCuTiS_3$, or the $TlCuTiTe_3$ structure type. Subtype II compounds, i.e. those of formula $A^{2+}M^{1+}M'^{3+}(Q^{2-})_3$, crystallize in either the $KCuZrS_3$, the Eu_2CuS_3, the Ba_2MnS_3, the $BaAgErS_3$, or the $BaCuLaS_3$ structure type. Subtype III compounds, i.e. those of formula $A^{1+}M^{2+}M'^{3+}(Q^{2-})_3$, crystallize in only the $KCuZrS_3$ structure type. Overall, the $KCuZrS_3$ structure type is by far the most common, with the Eu_2CuS_3 structure type the second most common. The remaining five structure types account for just 14 of the 160 compounds.

The $BaCuLaS_3$ and $BaAgErS_3$ structure types are channel structures. The other five structure types are layered and contain sheets of edge-sharing M'Q_6 or M'Q_7 polyhedra and MQ_4 tetrahedra separated by layers filled with rows of A atoms; the A atoms are coordinated by seven or eight chalcogen atoms. The relationship between the different structure types may be thought of as follows: The most symmetrical structure type is $KCuZrS_3$, which upon slight distortion of the layers becomes the Eu_2CuS_3 structure type. Upon further puckering of the layers, the structure becomes the Ba_2MnS_3 structure type. When the puckering is so great as to link the layers to each other

to form a three-dimensional channel structure, the $BaCuLaS_3$ structure type results. When the pattern of alternating tetrahedra and octahedra of the $KCuZrS_3$ structure type is doubled to alternating pairs of polyhedra, the $TlCuTiTe_3$ structure type is formed. Reversing every other layer turns the $TlCuTiTe_3$ structure type into the $NaCuTiS_3$ structure type. Lastly, the $BaAgErS_3$ structure type, which is a channel structure, has few aspects in common with any of the other structure types.

$KCuZrS_3$ Structure Type

In the $KCuZrS_3$ structure type (Figure 1A), $^2_\infty[MM'Q_3^-]$ layers align perpendicular to [010] and are separated by linear rows of A atoms in the [100] direction. Each $^2_\infty[MM'Q_3^-]$ layer comprises MQ_4 tetrahedra and $M'Q_6$ octahedra.

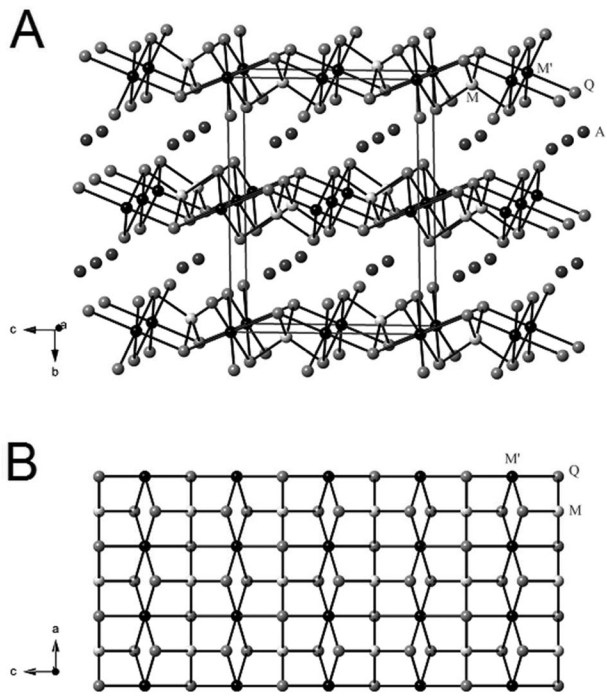

Figure 1. (A) The $KCuZrS_3$ structure type with the unit cell outlined. (B) View of one layer.

There are five crystallographically unique atoms: A, M, M', Q1, and Q2. Each M atom is coordinated by two Q1 and two Q2 atoms and each M' atom is coordinated by four equatorial Q1 and two axial Q2 atoms. Along the [001] direction, the $^2_\infty[MM'Q_3^-]$ layer comprises alternating edge-sharing MQ_4 and $M'Q_6$ polyhedra, whereas along the [100] direction the layer is composed of vertex-sharing tetrahedra and edge-sharing octahedra (Figure 1B). Each A atom is surrounded by eight Q atoms in a bicapped trigonal-prismatic arrangement.

The $KCuZrS_3$ structure type can be derived from the $PuBr_3$ structure type by way of the $ScUS_3$ structure type. Substitution of uranium for plutonium, and sulfur for bromine, and filling all of the octahedral sites with scandium results in the $ScUS_3$ structure type. Substitution of potassium for uranium, and zirconium for scandium, and filling one third of the tetrahedral sites with copper results in the $KCuZrS_3$ structure type.[1,25,26]

Eu_2CuS_3 Structure Type

The Eu_2CuS_3 structure type (i.e. $Eu^{2+}CuEu^{3+}S_3$) is a slightly distorted version of the $KCuZrS_3$ structure type. In the Eu_2CuS_3 structure type (Figure 2A), $^2_\infty[MM'Q_3^-]$ layers stack in an A/B/A/B fashion along [001]. These layers are separated by linear rows of A atoms in the [010] direction. Each $^2_\infty[MM'Q_3^-]$ layer comprises MQ_4 tetrahedra and $M'Q_6$ octahedra.

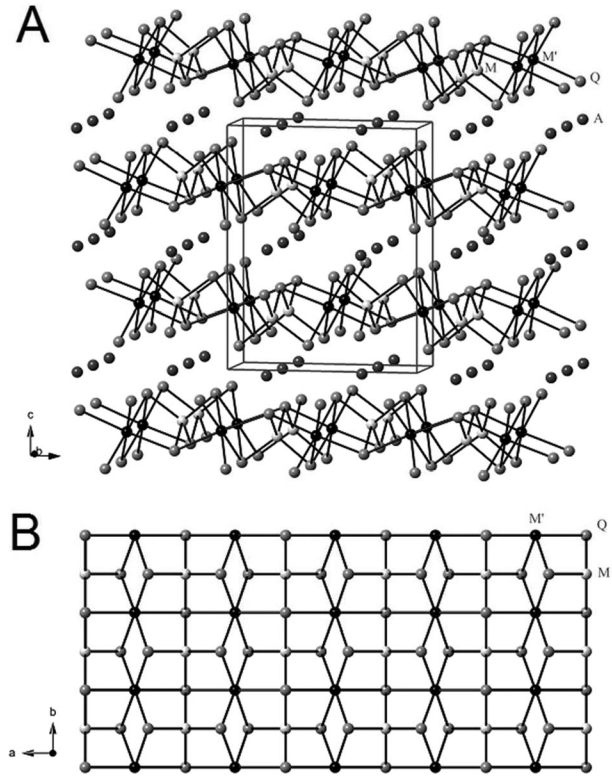

Figure 2. (A) The Eu_2CuS_3 structure type with the unit cell outlined. (B) View of one layer.

There are six crystallographically unique atoms: A, M, M', Q1, Q2, and Q3. Each M atom is coordinated by two Q1, one Q2, and one Q3 atom and each M' atom is coordinated by two atoms each of Q1, Q2, and Q3. Along the [100] direction, the $^2_\infty[MM'Q_3^-]$ layer is composed of alternating edge-sharing MQ_4 and $M'Q_6$ polyhedra, whereas along the [010] direction the layer is composed of vertex-sharing tetrahedra and edge-sharing octahedra (Figure 2B). Each A atom is surrounded by seven Q atoms in a monocapped trigonal-prismatic arrangement.

Ba_2MnS_3 Structure Type

In the Ba_2MnS_3 structure type (Figure 3A), highly puckered $^2_\infty[AMQ_3^{2-}]$ layers stack in an A/B/A/B fashion along [001]. These layers are separated by linear rows of A atoms in the [010] direction. Each $^2_\infty[AMQ_3^{2-}]$ layer comprises MQ_4 distorted tetrahedra and AQ_7 monocapped trigonal prisms.

Zeitschrift für anorganische und allgemeine Chemie ZAAC Journal of Inorganic and General Chemistry

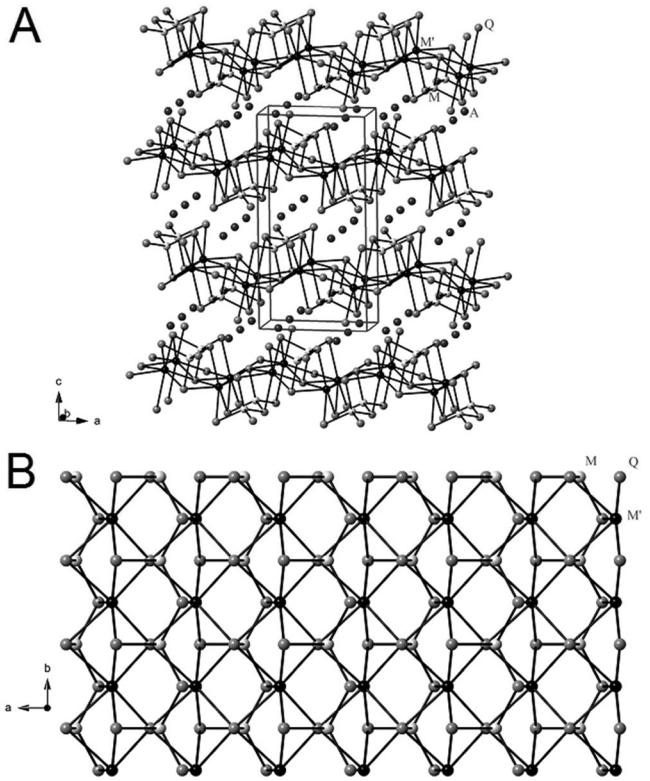

Figure 3. (A) The Ba_2MnS_3 structure type with the unit cell outlined. (B) View of one layer.

There are six crystallographically unique atoms: A1, A2, M, Q1, Q2, and Q3. Each M atom is coordinated by one Q1, one Q2, and two Q3 atoms and each A1 atom is coordinated by four Q1, two Q2, and one Q1 atom. Along the [100] direction, the $^2_\infty$[M(A1)Q_3^{2-}] layer is composed of alternating edge-sharing MQ_4 distorted tetrahedra and (A1)Q_7 monocapped trigonal prisms, whereas along the [010] direction, the layer is composed of vertex-sharing distorted tetrahedra and edge-sharing monocapped trigonal prisms (Figure 3B). Each A2 atom is surrounded by seven Q atoms in a monocapped trigonal-prismatic arrangement.

Only the three compounds SrCuM'Se_3 (M' = La, Ce)[27,28] and $PbCuLaS_3$[29] crystallize in this structure type. The Sr and M' atoms are disordered nearly equally over the A1 and A2 positions whereas the Pb and La are disordered over the A1 and A2 positions in an approximate 2:1 ratio.

The Ba_2MnS_3 structure type can be derived from the La_2S_3 structure type by substituting Ba for La and inserting Mn into half of the tetrahedral sites found in La_2S_3.[29]

$BaCuLaS_3$ Structure Type

The $BaCuLaS_3$ structure type (Figure 4A) can be thought of as being composed of layers of MQ_4 tetrahedra and M'Q_7 monocapped trigonal prisms stacked perpendicular to [001] where the M'Q_7 polyhedra cross-link between the layers to form a channel structure. The channels run along the [010] direction and are each filled with two rows of A atoms.

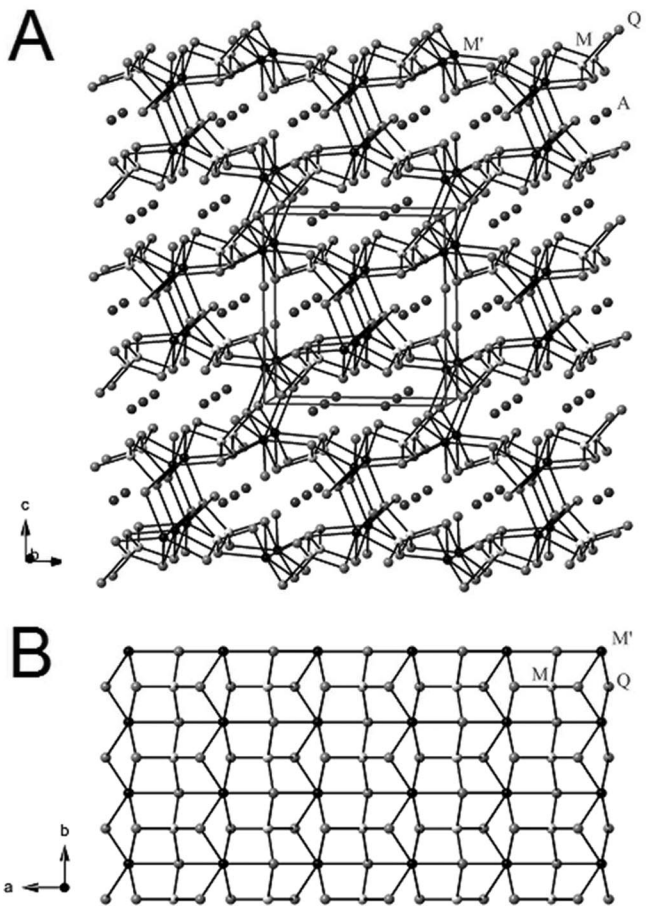

Figure 4. (A) The $BaCuLaS_3$ structure type with the unit cell outlined. (B) View of one layer.

There are six crystallographically unique atoms: A, M, M', Q1, Q2, and Q3. Each M atom is coordinated by two Q1, one Q2, and one Q3 atom and each M' atom is coordinated by two Q1, three Q2, and two Q3 atoms. Along the [100] direction, the MQ_4 tetrahedra and M'Q_7 monocapped trigonal prisms edge share with each other, whereas along the [010] direction the layer is composed of vertex-sharing tetrahedra and edge-sharing monocapped trigonal prisms (Figure 4B). There are two rows of A atoms in each channel and each A atom is coordinated by seven Q atoms in a monocapped trigonal-prismatic arrangement.

This structure type is only displayed by the compounds $BaCuLaS_3$[4] and α-$BaCuLaSe_3$.[12]

$BaAgErS_3$ Structure Type

The $BaAgErS_3$ structure type (Figure 5A) consists of pairs of M'Q_6 octahedra that share edges in a zigzag manner to form a double chain along the [010] direction (Figure 5B). The double chains corner share with each other to form $^2_\infty$[M'$_2Q_5^{4-}$] layers, which are further connected through pairs of corner-sharing M_2Q_9 trigonal bipyramids. A three-dimensional network is formed with channels along the [010] direction occupied by two rows of A atoms. Each A atom is coordinated by

seven Q atoms in a monocapped trigonal-prismatic arrangement.

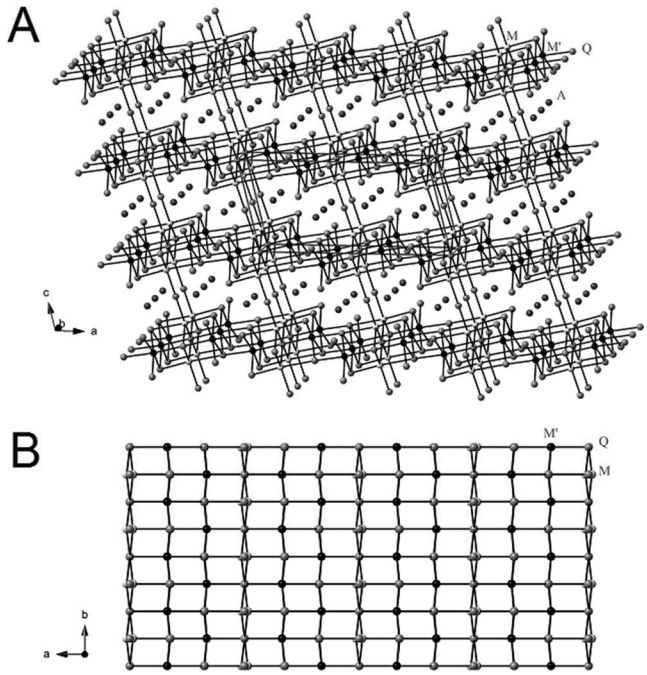

Figure 5. (A) The $BaAgErS_3$ structure type with the unit cell outlined. (B) View of one layer.

There are seven crystallographically unique atoms: A, M, M', Q1, Q2, Q3, and Q4. Each M atom is coordinated by one Q1, one Q2, one Q3, and two Q4 atoms and each M' atom is coordinated by three Q1, two Q2, and one Q4 atom.

Only the three compounds $BaAgM'S_3$ (M' = Y, Gd, Er)[5] crystallize in this structure type.

The $BaAgErS_3$ structure type is related to the $AgErSe_2$ structure type. The same $M'Q_6$ octahedral layers are found in both structures, but in $AgErSe_2$ two sets of such layers intersect to form a three-dimensional structure. Insertion of A^{2+} into the $AgErSe_2$ structure separates the layers and results in the $BaAgErS_3$ structure type.[5]

$NaCuTiS_3$ Structure Type

In the $NaCuTiS_3$ structure type (Figure 6A), $^2_\infty[MM'Q_3^-]$ layers stack in an A/B/A/B manner along [100] and are separated by linear rows of A atoms in the [010] direction. Each $^2_\infty[MM'Q_3^-]$ layer comprises MQ_4 tetrahedra and $M'Q_6$ octahedra.

There are six crystallographically unique atoms: A, M, M', Q1, Q2, and Q3. Each M atom is coordinated by three Q2 and one Q3 atom and each M' atom is coordinated by three Q1, one Q2, and two Q3 atoms. Along the [001] direction the $^2_\infty[MM'Q_3^-]$ layer is composed of alternating pairs of edge-sharing MQ_4 and pairs of edge-sharing $M'Q_6$ polyhedra, whereas along the [010] direction the layer is composed of alternating double chains of edge-sharing tetrahedra and edge-sharing octahedra (Figure 6B). Each A atom is surrounded by

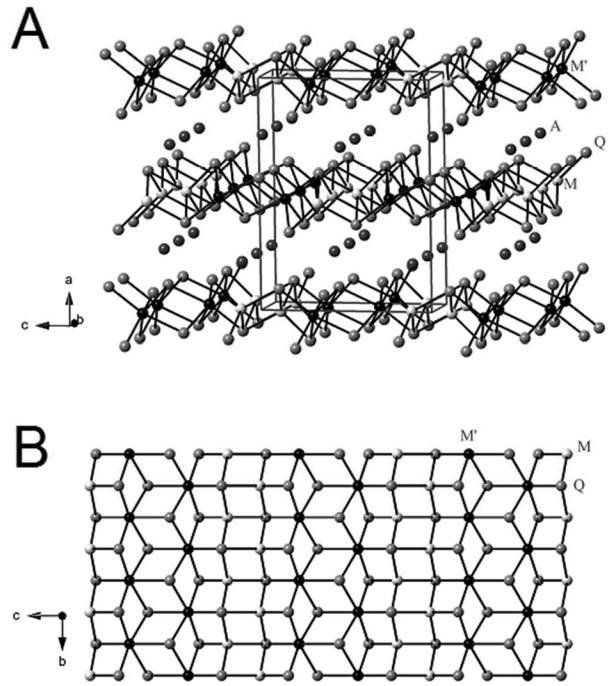

Figure 6. (A) The $NaCuTiS_3$ structure type with the unit cell outlined. (B) View of one layer.

seven Q atoms in a monocapped trigonal-prismatic arrangement.

$TlCuTiTe_3$ Structure Type

The $TlCuTiTe_3$ structure type (Figure 7A) is composed of $^2_\infty[MM'Q_3^-]$ layers that stack along the [101] direction; these layers align in an approximate A/B/C/A/B/C manner and are separated by linear rows of A atoms in the [010] direction. Each $^2_\infty[MM'Q_3^-]$ layer is composed of MQ_4 tetrahedra and $M'Q_6$ octahedra.

There are six crystallographically unique atoms: A, M, M', Q1, Q2, and Q3. Each M atom is coordinated by three Q2 and one Q3 atom and each M' atom is coordinated by three Q1, one Q2, and two Q3 atoms. The $^2_\infty[MM'Q_3^-]$ layer is composed of alternating pairs of edge-sharing MQ_4 and pairs of edge-sharing $M'Q_6$ polyhedra along the [101] direction, whereas along the [010] direction the layer is composed of alternating zigzags of edge-sharing tetrahedra and edge-sharing octahedra (Figure 7B). Each A atom is surrounded by seven Q atoms in a monocapped trigonal-prismatic arrangement.

In the$TlCuTiTe_3$ structure type (monoclinic) the pairs of polyhedra point in the same direction in each layer, whereas in the $NaCuTiS_3$ structure type (orthorhombic) the pairs of polyhedra point in alternating directions in each layer.

Relationships among the $KCuZrS_3$, Eu_2CuS_3, and Ba_2MnS_3 Structure Types

The compounds represented by the structure types $KCuZrS_3$ (space group *Cmcm*), Eu_2CuS_3 (space group *Pnma*), and

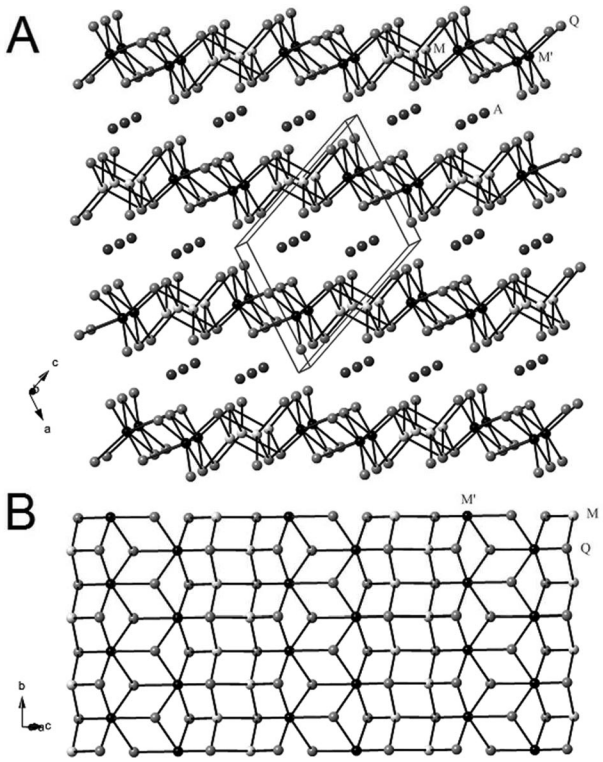

Figure 7. (A) The $TlCuTiTe_3$ structure type with the unit cell outlined. (B) View of one layer.

Ba_2MnS_3 (space group *Pnma*) all crystallize in the orthorhombic system. In the $KCuZrS_3$ structure type, the M' atom is coordinated by six Q atoms in an octahedral arrangement whereas the A atom is coordinated by eight Q atoms in a bicapped trigonal-prismatic arrangement. In the Eu_2CuS_3 structure type, the M' atom retains a coordination number of six whereas the A atom expands its coordination to accommodate a seventh Q atom. The increased coordination number necessitates the lowering of symmetry with atoms moving off of some special positions of space group *Cmcm*. The atomic rearrangement does not have a large effect on the unit cell lattice parameters; the value of *a*, *b*, and *c* for the $KCuZrS_3$ structure type by convention correspond to *b*, *c*, and *a* for the Eu_2CuS_3 structure type. In the Ba_2MnS_3 structure type, both the A1 and A2 atoms have coordination numbers of seven with disorder between A and M' atoms on both sites. This causes a puckering of the layers (compare Figure 2 with Figure 3) and a change in lattice parameters; *a* is longer in Eu_2CuS_3 than in Ba_2MnS_3, *b* remains the same, and *c* is shorter in in Eu_2CuS_3 than in Ba_2MnS_3.

Trends in Structure Types

Here we examine the different trends in structure types seen in the three subtypes of the structurally characterized AMM'Q_3 compounds. We emphasize that the AMM'Q_3 compounds that are known do not represent a random statistical sampling of the many possible compounds. Rather they reflect the interests of the various researchers or possibly unexpected products isolated on the way to other target compounds. The trends we discern are consequently based on a limited number of compounds; to corroborate these trends would require further synthetic and structural efforts.

There are, of course, electronic differences among the various M, M', and Q elements involved in the AMM'Q_3 compounds. For example, the actinides are generally believed to exhibit more covalency than do the lanthanides, at least in organometallic systems.[30] Such electronic differences could apply to solid-state compounds as well and affect the structure type in which a given AMM'Q_3 compound would crystallize. However, these compounds contain no Q–Q bonds and accordingly they charge balance with the expected formal oxidation states. As a result, we ignore electronic factors and consider only steric factors. We also assume that because the compounds were obtained after slow cooling they are the thermodynamic products. The crystal radii[31] for all the elements found in the structurally characterized AMM'Q_3 compounds are listed in Table 4 because the trends we discern depend on these radii.

Table 4. Crystal radii[a] of elements in the compounds AMM'Q_3. The A, M, M', and Q elements are arranged in order of increasing crystal radii.

A (CN)	radius/Å	M' (CN)	radius/Å	Q (CN)	radius/Å
Na^+ (VIII)	1.32	Sc^{3+} (VI)	0.885	S^{2-} (VI)	1.70
K^+ (VIII)	1.65	Lu^{3+} (VI)	1.001	Se^{2-} (VI)	1.84
Tl^+ (VIII)	1.73	Yb^{3+} (VI)	1.008	Te^{2-} (VI)	2.07
Rb^+ (VIII)	1.75	Tm^{3+} (VI)	1.020	M (CN)	radius/Å
Cs^+ (VIII)	1.88	Er^{3+} (VI)	1.030	Cu^+ (IV)	0.74
Eu^{2+} (VII)	1.34	Y^{3+} (VI)	1.040	Ag^+ (IV)	1.14
Sr^{2+} (VII)	1.35	Ho^{3+} (VI)	1.041	Au^+ (IV)	[b]
Pb^{2+} (VII)	1.37	Dy^{3+} (VI)	1.052	Zn^{2+} (IV)	0.74
Ba^{2+} (VII)	1.52	Tb^{3+} (VI)	1.063	Mn^{2+} (IV)	0.80
M' (CN)	radius/Å	Gd^{3+} (VI)	1.078	Hg^{2+} (IV)	0.83
Ti^{4+} (VI)	0.88	Eu^{3+} (VI)	1.087	Cd^{2+} (IV)	0.92
Hf^{4+} (VI)	0.97	Sm^{3+} (VI)	1.098		
Zr^{4+} (VI)	0.98	Nd^{3+} (VI)	1.123		
Np^{4+} (VI)	1.12	Pr^{3+} (VI)	1.13		
U^{4+} (VI)	1.14	Ce^{3+} (VI)	1.15		
Th^{4+} (VI)	1.19	La^{3+} (VI)	1.172		

a) Ref. [31]. b) No crystal radius is listed in Ref. [31] for tetrahedrally coordinated Au^{1+}, but its radius is presumably the same or smaller than that of Ag^{1+}. For example, in Na_3AgS_2 the Ag–S distance is 2.37 Å [45] whereas in Na_3AuS_2 the Au–S distance is 2.30 Å.[46] However, the compounds are not isostructural.

Thirty-three of the 39 subtype I compounds, $A^{1+}M^{1+}M'^{4+}Q^{2-}$, are of the $KCuZrS_3$ structure type. All actinide compounds crystallize in the $KCuZrS_3$ structure type. Of the six subtype I compounds not crystallizing in the $KCuZrS_3$ structure type four have A = Na. This suggests that the smallest of the A atoms largely determines the structure. However, $NaCuZrS_3$ crystallizes in the $KCuZrS_3$ structure type, possibly because of the larger zirconium atom. Substitution of sulfur for selenium returns the structure to the $NaCuTiS_3$ type, an indication that zirconium is not large in combination with selenium. The remaining two exceptions to the $KCuZrS_3$ structure type are the compounds $RbAgHfTe_3$ and $TlCuTiTe_3$, which both crystallize in the $TlCuTiTe_3$ structure type. Note that $RbAuUTe_3$ crystallizes in the $KCuZrS_3$ structure type and that uranium is larger than hafnium. This situation is analogous to the one for the $NaCuTiS_3$/$NaCuZrS_3$ pair; the structural motif of pairs of alternating polyhedra in the $TlCuTiTe_3$ structure type is very similar to the one in the $NaCuTiS_3$ structure type.

All the 63 subtype II compounds, $A^{2+}M^{1+}M'^{3+}Q^{2-}$, are lanthanides (M'). All but eight of these are of either the $KCuZrS_3$ or Eu_2CuSe_3 structure types, with the eight compounds falling into three additional structure types, namely the Ba_2MnS_3, the $BaAgErS_3$, or the $BaCuLaS_3$ structure types. For the $SrCuM'Q_3$ compounds the smallest M' (Lu) crystallizes in the $KCuZrS_3$ structure type, intermediate sized M' (Gd, Pr) crystallize in the Eu_2CuSe_3 structure type, and largest M' (Ce, La) crystallize in the Ba_2MnS_3 structure type. There is no variation in structure type on going from sulfur to selenium. The $EuCuM'S_3$ compounds are of the $KCuZrS_3$ structure type for the smaller M' (Lu, Yb, Tm) and of the Eu_2CuSe_3 structure type for the larger M' (Y, Dy, Tb, Gd, Eu). Clearly, in these systems the size of M' determines the structure type. The three that crystallize in the $BaAgErS_3$ type, namely $BaAgM'S_3$ (M' = Er, Y, Gd), show a dependence on M, as the $BaCuM'S_3$ compounds crystallize in the $KCuZrS_3$ structure type. For $PbCuM'Q_3$, the compounds are of the Eu_2CuSe_3 structure type when Q = Se, whereas all but two are of the $KCuZrS_3$ structure type when Q = S; hence the size of Q plays a role in this series. When arranged in order of increasing size of M', all $PbCuM'Q_3$ compounds up to M' = La (with the apparent exception of M' = Y, as determined from X-ray diffraction powder data contaminated with $YCuS_2$ and PbS[32]) are of the $KCuZrS_3$ structure type, but $PbCuLaS_3$ is of the Ba_2MnS_3 structure type, again indicating a dependence of structure type on M'. The $BaCuM'S_3$ compounds crystallize in different structure types, again depending on the size of M'. The smaller M' (Sc, Er, Y, Gd) crystallize in the $KCuZrS_3$ structure type, the intermediate-sized M' (Nd, Ce) crystallize in the Eu_2CuS_3 structure type, and the largest M' (La) crystallizes in the $BaCuLaS_3$ structure type. The compound $BaCuLaSe_3$ has two polymorphs, namely the β form, which crystallizes in the layered the Eu_2CuSe_3 structure type, and the high-pressure, more dense α form, which crystallizes in the channel $BaCuLaS_3$ structure type. Only the α form is known for $BaCuLaSe_3$.[4,12]

All 58 subtype III compounds, $A^{1+}M^{2+}M'^{3+}Q^{2-}$, are of the $KCuZrS_3$ structure type regardless of the crystal radii of the constituent elements. All are lanthanides (M'). Within these subtype II compounds there is only one Q = S; the others have Q = Se or Te. Only two have A = Rb; the others have A = Cs. Thus, there are many gaps, and other structure types may be discovered in the future if one invokes greater variation in crystal radii, especially among the A constituents of subtype III compounds.

Conclusions

There are 160 structurally characterized compounds of the type $AMM'Q_3$. As large as that number seems, the vast majority of possible $AMM'Q_3$ compounds have yet to be synthesized and characterized. In fact, the possible number of the combinations of elements that are present in the 160 known compounds (Table 4) is 1806. Even more compounds are possible if one considers analogues that currently have no precedents, e.g., those containing lithium and calcium for A or plutonium for M'. The physical characterization of these compounds lags as well; only 63 of the 160 known compounds have been subjected to some sort of physical measurement.

Here we have examined the structural differences among the 160 characterized $AMM'Q_3$ compounds. In doing so, we have ignored possible electronic factors and considered only steric factors. We also assume that the compounds so examined are thermodynamic products. We find that the trends we discern in the structures of these compounds can largely be rationalized on the basis of the crystal radii of the constituent atoms.

Supporting Information (see footnote on the first page of this article): Tables S1 and S2 in color.

Acknowledgment

The research was supported at Northwestern University by the U.S. Department of Energy, Basic Energy Sciences, Chemical Sciences, Biosciences, and Geosciences Division and Division of Materials Sciences and Engineering Grant ER-15522. LAK was also supported by the Nuclear Energy University Programs of the U.S. Department of Energy Office of Nuclear Energy.

References

[1] M. F. Mansuetto, P. M. Keane, J. A. Ibers, *J. Solid State Chem.* **1992**, *101*, 257–264.
[2] P. Lemoine, D. Carré, M. Guittard, *Acta Crystallogr., Sect. C* **1986**, *42*, 390–391.
[3] I. E. Grey, H. Steinfink, *Inorg. Chem.* **1971**, *10*, 691–696.
[4] A. E. Christuk, P. Wu, J. A. Ibers, *J. Solid State Chem.* **1994**, *110*, 330–336.
[5] P. Wu, J. A. Ibers, *J. Solid State Chem.* **1994**, *110*, 156–161.
[6] M. F. Mansuetto, P. M. Keane, J. A. Ibers, *J. Solid State Chem.* **1993**, *105*, 580–587.
[7] M. A. Pell, J. A. Ibers, *J. Alloys Compd.* **1996**, *240*, 37–41.
[8] S. A. Sunshine, D. Kang, J. A. Ibers, *J. Am. Chem. Soc.* **1987**, *109*, 6202–6204.
[9] A. C. Sutorik, J. Albritton-Thomas, T. Hogan, C. R. Kannewurf, M. G. Kanatzidis, *Chem. Mater.* **1996**, *8*, 751–761.
[10] D. E. Bugaris, J. A. Ibers, *J. Solid State Chem.* **2009**, *182*, 2587–2590.
[11] M. Wakeshima, F. Furuuchi, Y. Hinatsu, *J. Phys.: Condens. Matter* **2004**, *16*, 5503–5518.

[12] P. Wu, A. E. Christuk, J. A. Ibers, *J. Solid State Chem.* **1994**, *110*, 337–344.
[13] F. Q. Huang, K. Mitchell, J. A. Ibers, *Inorg. Chem.* **2001**, *40*, 5123–5126.
[14] Y. Yang, J. A. Ibers, *J. Solid State Chem.* **1999**, *147*, 366–371.
[15] K. Mitchell, F. Q. Huang, E. N. Caspi, A. D. McFarland, C. L. Haynes, R. C. Somers, J. D. Jorgensen, R. P. Van Duyne, J. A. Ibers, *Inorg. Chem.* **2004**, *43*, 1082–1089.
[16] K. Mitchell, C. L. Haynes, A. D. McFarland, R. P. Van Duyne, J. A. Ibers, *Inorg. Chem.* **2002**, *41*, 1199–1204.
[17] Y. Liu, L. Chen, L.-M. Wu, G. H. Chan, R. P. Van Duyne, *Inorg. Chem.* **2008**, *47*, 855–862.
[18] K. Mitchell, F. Q. Huang, A. D. McFarland, C. L. Haynes, R. C. Somers, R. P. Van Duyne, J. A. Ibers, *Inorg. Chem.* **2003**, *42*, 4109–4116.
[19] J. Yao, D. M. Wells, G. H. Chan, H.-Y. Zeng, D. E. Ellis, R. P. Van Duyne, J. A. Ibers, *Inorg. Chem.* **2008**, *47*, 6873–6879.
[20] H. D. Selby, B. C. Chan, R. F. Hess, K. D. Abney, P. K. Dorhout, *Inorg. Chem.* **2005**, *44*, 6463–6469.
[21] J. Yao, B. Deng, L. J. Sherry, A. D. McFarland, D. E. Ellis, R. P. Van Duyne, J. A. Ibers, *Inorg. Chem.* **2004**, *43*, 7735–7740.
[22] F. Q. Huang, J. A. Ibers, *Inorg. Chem.* **2001**, *40*, 2602–2607.
[23] J. Hafner, *J. Comput. Chem.* **2008**, *29*, 2044–2078.
[24] P. Blaha, K. Schwarz, G. K. Madsen, D. Kvasnicka, J. Luitz, *WIEN2k*, An Augmented Plane Wave + Local Orbitals Program for Calculating Crystal Properties; Karlheinz Schwarz, Techn. Universität Wien, Vienna, Austria, **2001**.
[25] L. D. Gulay, I. D. Olekseyuk, M. Wolcyrz, J. Stepien-Damm, *J. Alloys Compd.* **2005**, *399*, 189–195.
[26] J. A. Cody, J. A. Ibers, *Inorg. Chem.* **1995**, *34*, 3165–3172.
[27] S. Strobel, Th. Schleid, *J. Alloys Compd.* **2006**, *418*, 80–85.
[28] S. Strobel, Th. Schleid, *Z. Naturforsch.* **2004**, *59b*, 985–991.
[29] T. D. Brennan, J. A. Ibers, *J. Solid State Chem.* **1992**, *97*, 377–382.
[30] A. J. Gaunt, S. D. Reilly, A. E. Enriquez, B. L. Scott, J. A. Ibers, P. Sekar, K. I. M. Ingram, N. Kaltsoyannis, M. P. Neu, *Inorg. Chem.* **2008**, *47*, 29–41.
[31] R. D. Shannon, *Acta Crystallogr., Sect. A* **1976**, *32*, 751–767.
[32] L. D. Gulay, V. Y. Shemet, I. D. Olekseyuk, *J. Alloys Compd.* **2005**, *388*, 59–64.
[33] K. O. Klepp, D. Sturmayr, *Z. Kristallogr. NCS* **1997**, *212*, 75.
[34] K. O. Klepp, D. Sturmayr, *Z. Kristallogr. NCS* **1998**, *213*, 693.
[35] D. M. Wells, G. B. Jin, S. Skanthakumar, R. G. Haire, L. Soderholm, J. A. Ibers, *Inorg. Chem.* **2009**, *48*, 11513–11517.
[36] A. A. Narducci, J. A. Ibers, *Inorg. Chem.* **2000**, *39*, 688–691.
[37] K. O. Klepp, D. Gurtner, *J. Alloys Compd.* **1996**, *243*, 6–11.
[38] L. A. Koscielski, J. A. Ibers, *Acta Crystallogr., Sect. E* **2012**, *68*, i52–i53.
[39] M. A. Pell, A. G. Kleyn, J. A. Ibers, *Z. Kristallogr. NCS* **1997**, *212*, 92.
[40] N. V. Sikerina, O. V. Andreev, *Russ. J. Inorg. Chem. (Transl. of Zh. Neorg. Khim.)* **2007**, *52*, 581–584.
[41] L. D. Gulay, I. D. Olekseyuk, *J. Alloys Compd.* **2005**, *387*, 160–164.
[42] L. D. Gulay, D. Kaczorowski, A. Pietraszko, *J. Alloys Compd.* **2006**, *413*, 26–28.
[43] L. D. Gulay, V. Y. Shemet, I. D. Olekseynuk, *J. Alloys Compd.* **2004**, *385*, 160–168.
[44] F. Q. Huang, W. Choe, S. Lee, J. S. Chu, *Chem. Mater.* **1998**, *10*, 1320–1326.
[45] K. O. Klepp, W. Bronger, *J. Less-Common Met.* **1985**, *106*, 95–101.
[46] K. O. Klepp, W. Bronger, *J. Less-Common Met.* **1987**, *132*, 173–179.

Received: June 27, 2012
Published Online: September 7, 2012

Special Issue

